Progress In Electromagnetics Research C, Vol. 46, 31–39, 2014

Design and Analysis of New Compact UWB Frequency Selective Surface and Its Equivalent Circuit

Nagendra Kushwaha[1], Raj Kumar[2, *], Raghupatruni V. S. Ram Krishna[1], and Tuhina Oli[1]

Abstract—A compact, low profile, dual polarized, ultra wideband, frequency selective surface is proposed. It is designed by using two similar metallic array structures separated by dielectric material FR4. The simulated reflection bandwidth (with transmission < -20 dB) for TE incident wave is 8 GHz from 2.87 GHz to 10.87 GHz corresponds to 116%. The unit cell dimension and periodicity are of the order of 0.37λ at the centre frequency. The overall thickness of the proposed FSS is 1.8 mm. The proposed FSS has higher order of band-stop response and good angular stability. The measured transmission response of FSS is very close to simulated response. Design expressions for the resonance frequencies are proposed, and the calculated results are found to be in good agreement with the simulated ones. Finally, a parametric analysis of the proposed FSS is presented.

1. INTRODUCTION

High Impedance Surfaces (HISs) or Artificial Magnetic Conductors (AMCs) are very popular among researchers for variety of applications in microwave circuits. Earlier, conventional ground planes made of good conducting material were used as reflectors and to provide shielding for electronics beneath the antenna. But the conventional ground plane has some drawbacks such as introduction of image current in the opposite direction to the source which is placed above the ground plane. If the ground plane is used as a reflector and the antenna is placed very near to the ground plane, there will be current cancellation of the source antenna with its image. This results in poor impedance matching and poor radiation efficiency. On the other hand, AMCs and HISs not only provide the shielding to electronics beneath the antenna but also redirect the wave in one direction. As the AMCs give an image current which is in phase with the source current horizontally placed above, there is greater impedance matching. Hence, the impedance bandwidth of the antenna is improved after application of AMCs [1–3]. The HISs and AMCs are also known as Electromagnetic Band Gap (EBG) structures and Frequency Selective Surfaces (FSS). FSSs are used to enhance the impedance bandwidth and gain of an antenna [4–7]. In addition, FSS superstrate is also used as a polarizer to get circular polarization in case of single source excitation and it can also rotate the linearly polarized waves by 90° in a given frequency band [8–11].

The characteristics of FSSs are determined by the shape, size and the spacing between unit elements. Various shapes have been designed and analyzed in the past. FSS shapes can be classified as centre connected, solid interior, loop type and the combination of all these. All the above shapes are having the disadvantage of low transmission bandwidth for incident TE waves which limits their applications. To overcome this limitation, multilayer FSS structures have been introduced. The advantage of multilayer FSS structures is wider bandwidth. To achieve higher order transmission response, multiple layers of FSS arrays are cascaded with quarter wavelength spacing between each layer. The problem with these types of FSS structures is that they are not suited for conformal applications requiring covering structures with moderate to small radii of curvature. Moreover, the size of FSS structure becomes very

Received 9 October 2013, Accepted 10 December 2013, Scheduled 12 December 2013

* Corresponding author: Raj Kumar (raj34_shivani@yahoo.co.in).

[1] Research Scholar DIAT (DU), Pune 411025, India. [2] ARDE, Pashan, Pune 411021, India.

bulky at lower frequencies and also angle sensitivity of the response increases. The loop type FSS is considered to be wideband FSS. An Ultra Wideband (UWB) FSS can be designed using multilayer loop type FSS [12]. The analysis of loop type FSS has also been done using different approaches [13–17].

In this paper, a UWB FSS has been designed using modification of loop type FSS. The FSS array is printed on both sides of dielectric material of relative permittivity 4.4 and a compact, low profile UWB FSS is realized. The periodicity and dimensions of unit element is considerably smaller than the operating wavelength. This helps in reducing the sensitivity of the response to angle of incidence and reduces the grating lobes. The thickness of FSS presented in this paper is around $\lambda/23$ at centre frequency of 7 GHz which is considerably small as compared to conventional multilayer FSS whose thickness is of the order of $\lambda/4$. The proposed FSS can have a variety of applications such as high reflection layers, shielding in ultra-wideband systems and gain and bandwidth enhancement of the antenna in devices such as ground penetrating radar. The orientation of this paper is such that, in second section the principle of operation and design of the FSS is discussed. In third section, simulated and measured responses are discussed. In fourth section, a parametric study of the FSS is presented. Finally conclusions are made.

2. PRINCIPLE OF OPERATION AND DESIGN OF FSS

2.1. Principle of Operation

Figure 1 shows the three dimensional view of the two metallic layers of the proposed FSS. The FSS structure is composed of a dielectric layer sandwiched between two metallic layers. Two layers of the screen help in achieving wider bandwidth and higher order response. The top and the bottom layer have a similar 2-D periodic arrangement of modified loop type patches. Each unit cell has maximum physical dimension of 16 mm which is nearly equal to the periodicity of the structure and it is smaller than the operating centre wavelength, therefore the sensitivity of response to the incident angle is reduced. The principle of operation can be better understood by considering equivalent circuit shown in Figure 2 which is valid for normal incidence. The loop type patches are modelled by a resonant circuit (combination of L_f and C_f). The dielectric material separating the two metallic layers is modelled by a short portion of transmission line with characteristic impedance Z_1 given by

$$Z_1 = Z_0/\sqrt{\varepsilon_r} \tag{1}$$

Here Z_0 is the free space impedance which is equal to 377 Ω. The half spaces on the two sides of (above and below) the FSS structure are modelled by a semi-infinite transmission line with characteristic impedance Z_0.

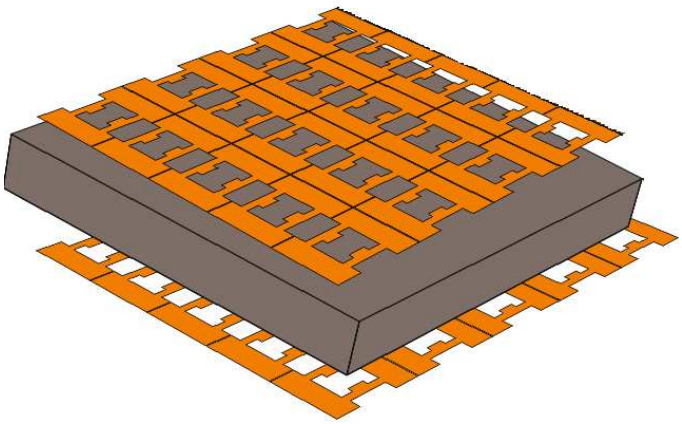

Figure 1. Three dimensional view of proposed FSS structure.

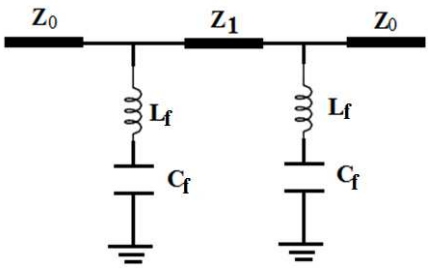

Figure 2. A simple equivalent circuit model for the proposed FSS.

2.2. Design of Frequency Selective Surface

The proposed FSS is designed by modifying a basic loop type structure such that the electrical length of the loop type element is increased and the width of loop remains nearly constant. The unit element of the proposed FSS is shown in Figure 3. The size of the unit element is 16 mm × 16 mm. Initially, the basic loop type structure is considered for analysis. It is found that the frequency of operation of the loop type structure heavily depends upon the overall size of the FSS element and the width forming the loop. The bandwidth of the loop type FSS depends upon the width of the metallic strip. A higher value of width will give higher bandwidth but the width should be limited to a particular value. The disadvantage of having higher value of width W is that the bandwidth shifts towards the higher frequency side.

In the proposed FSS structure, slots (of size $W_1 \times L_1$) have been cut from the loop type structure to have larger electrical length. Cutting slot in the loop type structure decreases the width of the loop and hence the bandwidth. To overcome this problem, small patches are added to the loop ($W_2 \times L_2$ as shown in Figure 3) such that the equivalent width remains nearly same and hence the bandwidth. Figure 4 shows a comparison of transmission characteristics of proposed FSS with conventional loop for single layer array of the same dimensions. It can be seen from the figure that the proposed FSS has lower resonance frequency as compared to conventional loop; therefore compactness is achieved in the case of proposed FSS. The bandwidth (Transmission < -20 dB) is nearly same for both the cases. To get the ultra wideband response, the proposed loop is printed on both sides of the substrate and the optimized dimensions are given in Table 1.

Figure 5 shows the simplified equivalent circuit of the proposed FSS. The lumped elements shown

Table 1. Optimized dimensions of unit element.

S. No.	Parameter	Dimension (mm)
1	W	4.20
2	L	4.50
3	W_1	2.40
4	L_1	7.00
5	W_2	1.20
6	L_2	3.00

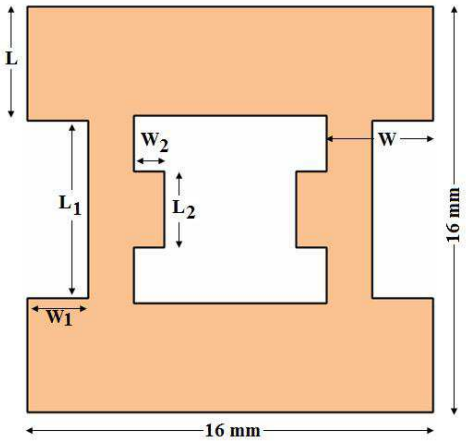

Figure 3. Unit cell of proposed FSS.

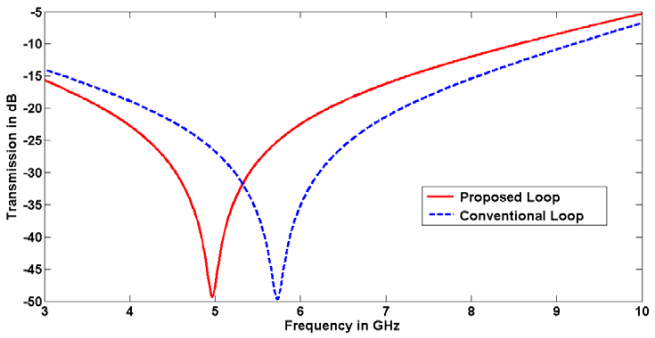

Figure 4. Comparison of transmission characteristics of proposed FSS with conventional loop for single layer array.

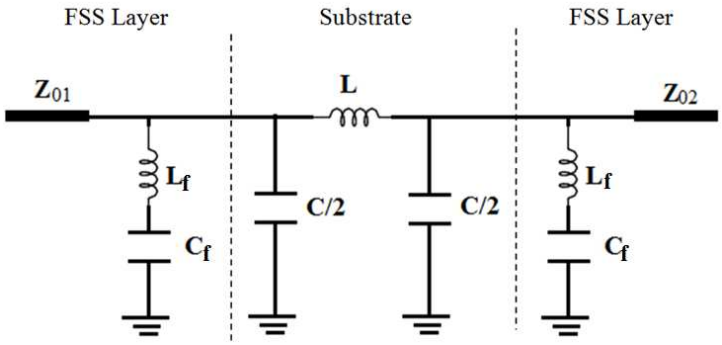

Figure 5. Simplified equivalent circuit model for proposed FSS shown in Figure 1.

in the figure, i.e., the inductance L and capacitance C are given by [17]

$$L = \mu_0 \mu_r h \tag{2}$$

$$C = \frac{\varepsilon_0 \varepsilon_r h}{2} \tag{3}$$

Here μ_0 is the permeability of the free space, μ_r is the relative permeability of the dielectric substrate used, h is the height of the dielectric substrate, ε_0 is the permittivity of the free space and ε_r is the relative permittivity of the dielectric substrate. The value of the inductance L_f and capacitance C_f can be approximated by considering the conventional loop and given by following relations [15, 18]

$$\frac{X_{L_f}}{Z_0} = \frac{d}{p} F_1(p, W, \lambda) \tag{4}$$

$$\frac{B_{C_f}}{Y_0} = 4\frac{d}{p} F_2(p, g, \lambda) \tag{5}$$

$$F_1(p, W, \lambda) = \frac{p}{\lambda}\left[\ln\left(\operatorname{cosec}\frac{\pi W}{2p}\right) + G_1(p, W, \lambda)\right] \tag{6}$$

$$F_2(p, g, \lambda) = \frac{p}{\lambda}\left[\ln\left(\operatorname{cosec}\frac{\pi g}{2p}\right) + G_2(p, g, \lambda)\right] \tag{7}$$

Here X_{Lf} is the reactance associated with L_f, B_{Cf} the susceptance associated with C_f, p the periodicity, d the size of unit element square, W the width of the loop, g the gap between two elements in the array, λ the operating wavelength, and ε_{eff} the effective permittivity. G_1 (p, W, λ) and G_2 (p, g, λ) are the correction factors for the associated inductance and capacitance respectively. The correction factors if ignored can cause minor deviation in the results. By using Equations (4), (5), (6) and (7), the value of L_f and C_f is found to be 2.96 nH and 0.351 pF respectively. The calculated values of lumped parameters are given in Table 2.

Table 2. Calculated values of lumped parameters.

S. No.	Parameter	Calculated Value
1	L	2.016 nH
2	C	0.031 pF
3	L_f	2.96 nH
4	C_f	0.351 pF

The lowest resonance frequency of the proposed double layer FSS can be approximated by solving the equivalent circuit model given in Figure 5 and it is given by f_l

$$f_l = \frac{1}{2\pi\sqrt{(L + L_f/2)(C + 2C_f)}} \tag{8}$$

By using Equation (8) and values given in Table 2, the lowest frequency of the proposed FSS screen is calculated as 3.15 GHz, which is close to simulated lowest resonance frequency of 3.00 GHz seen in Figure 8. The calculated resonance frequency is higher than the simulated frequency because conventional loop is considered for the calculation. The second resonance frequency (SRF) of the proposed FSS mainly depends upon the parameters L_1, L_2 and W_2. The SRF is curve fitted and given by

$$\text{SRF} = 6.56 + a\sin(-cL_1) + be^{cW_2} \tag{9}$$

$$a = -0.135L_2 - 0.4032 \tag{10}$$

$$b = 0.178L_2 - 0.1463 \tag{11}$$

$$c = -0.0143L_2 + 0.7138 \tag{12}$$

The SRF calculated from Equation (9) is in GHz with the values of L_1, L_2 and W_2 in mm. Also, Equation (9) is only valid when the substrate is having permittivity of 4.4 and thickness of 1.6 mm. The equation for the SRF is having a good level of accuracy. To verify the equation for the SRF, the simulated and calculated SRF (from Equation (9)) is compared for different values of parameters and is given in Table 3, Table 4 and Table 5. The simulated and calculated values of the SRF are very close to each other. The average deviation between the calculated value and the simulated value is 1.88%.

Table 3. Calculated and simulated SRF comparison for different values of W_2 ($L_1 = 3$ mm, $L_2 = 3$ mm).

S. No.	W_2 value (mm)	Calculated SRF (GHz)	Simulated SRF (GHz)	Deviation
1	0.8	7.95	7.62	4.33%
2	1.0	8.05	7.98	0.88%
3	1.2	8.16	8.22	0.72%
4	1.4	8.28	8.35	0.83%
5	1.6	8.42	8.65	2.65%

Table 4. Calculated and simulated SRF comparison for different values of L_1 ($L_2 = 3$ mm, $W_2 = 1.2$ mm).

S. No.	L_1 Value (mm)	Calculated SRF (GHz)	Simulated SRF (GHz)	Deviation
1	2	8.21	8.21	0%
2	3	8.15	8.22	0.85%
3	4	7.78	7.65	1.69%
4	5	7.25	7.26	0.13%
5	6	6.80	6.83	0.43%
6	7	6.62	6.68	0.89%

Table 5. Calculated and simulated SRF comparison for different values of L_2 ($L_1 = 7$ mm, $W_2 = 1.2$ mm).

S. No.	L_2 Value (mm)	Calculated SRF (GHz)	Simulated SRF (GHz)	Deviation
1	1	6.10	6.08	0.33%
2	2	6.37	6.22	2.41%
3	3	6.62	6.68	0.89%
4	4	6.87	6.86	0.15%

3. EXPERIMENTAL AND SIMULATED RESULTS

The characteristics of the proposed FSS are measured in an anechoic chamber. Two double ridge horn antennas are used as reference antennas. Figure 6 shows the block diagram of measurement setup used. The FSS is placed between the two horn antennas such that it is in the far field region of both the antennas. The FSS is illuminated by the plane waves generated by the transmitting horn antenna and the transmitted waves through the FSS are collected by the receiving horn antenna. The Vector Network Analyzer (VNA) is used to calculate the ratio of received signal strength to transmitted signal strength (S_{21}).

The FSS structure is optimized and fabricated. A photograph of fabricated FSS is shown in Figure 7. Figure 8 shows the measured and simulated transmission response of the proposed FSS for incident TE waves. The simulated (−20 dB transmission) bandwidth is 8 GHz from 2.87 GHz to 10.87 GHz. The measured transmission response follows the simulated response. The phase of the proposed FSS for incident TE waves is seen to be linearly decreasing. Figure 9 shows the measured and simulated transmission response of the proposed FSS for incident TM waves. The simulated (−20 dB transmission) bandwidth is 5 GHz from 3.27 GHz to 8.27 GHz. The bandwidth for both the cases (incident TE and TM) is not equal because the structure is not symmetrical with respect to 90° rotations.

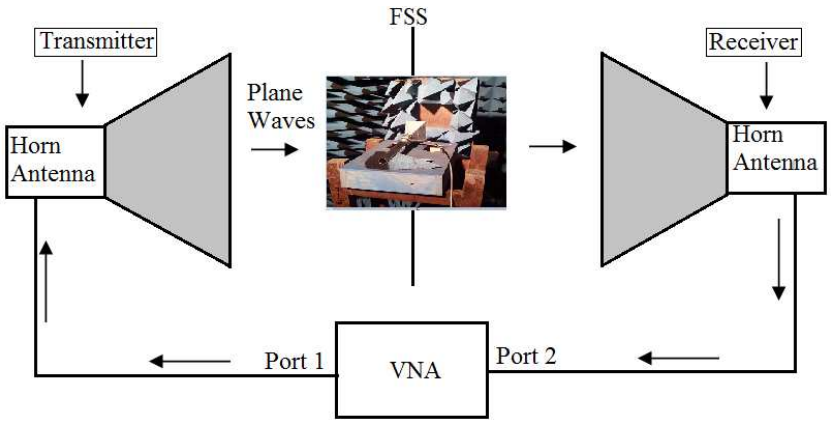

Figure 6. Block diagram of measurement setup.

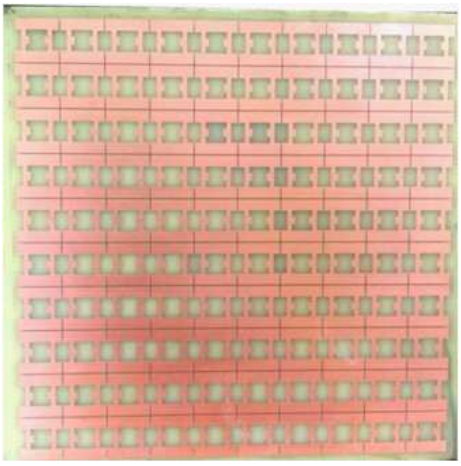

Figure 7. Fabricated prototype of proposed FSS.

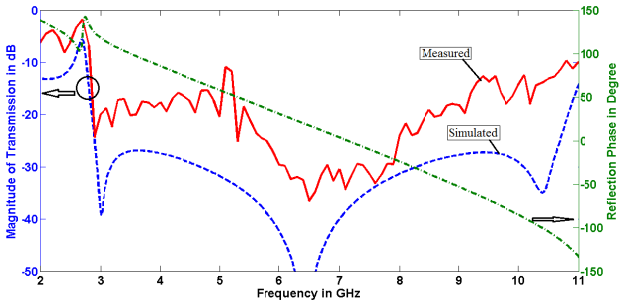

Figure 8. Measured and simulated transmission response of the proposed FSS for incident TE mode.

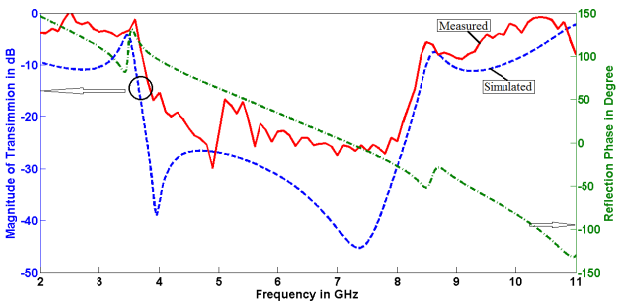

Figure 9. Measured and Simulated transmission response of the proposed FSS for incident TM mode.

4. PARAMETRIC ANALYSIS OF THE PROPOSED FSS

A parametric analysis is done to investigate the effects of different parameters on the response of the proposed FSS. Figure 10 shows the variation of transmission response of FSS with respect to the width of the loop W. From the figure, it can be seen that as the width W increases, the transmission band shifts towards the higher side due to decrease in the value of inductance L_1. The optimized value of W is found to be 4.2 mm. A further increase in the value of W results in band splitting. The values of other parameters are kept constant while varying the value of width W. The effect of the slot width W_1 on the transmission response is shown in Figure 11. It can be seen from the figure that as the width increases, the bandwidth shifts toward lower side and also decreases. The optimized value of W_1 is 2.4 mm.

Figure 12 shows the effect of variation of patch width W_2 on the transmission response. It can be seen from the figure that the variation of W_2 has little effect on the bandwidth but it certainly has an effect on the SRF. It can be seen from the figure that as the value of W_2 increases the SRF also increases. From Equation (9), it can be said that the SRF increases exponentially with an increase in the value of W_2. The effect of variation of slot length L_1 on the transmission response is shown in Figure 13. It can be seen from the figure, increasing the length L_1 increases the bandwidth up to a certain value ($L_1 = 7.0$ mm). After that, the bandwidth splits. The SRF decreases as the value of L_1 increases. From Equation (9), it can be said that the SRF decreases sinusoidally with an increase in the value of L_1. Figure 14 shows the effect of variation of patch length L_2 on the transmission response. It can be seen from the figure that increasing the length L_2 decreases the bandwidth. The SRF also depends upon the value of L_2. The value of SRF increases as the value of L_2 increases.

Figure 15 shows the effect of variation of incident angle on the transmission response of the proposed

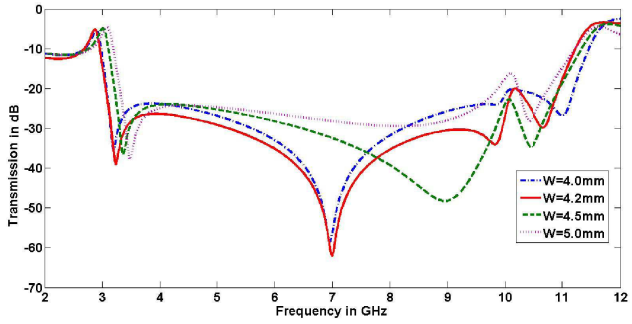

Figure 10. Effect of loop width W on the transmission response of FSS ($W_1 = 2.4$ mm, $L_1 = 3$ mm, $L_2 = 3$ mm, $W_2 = 1$ mm).

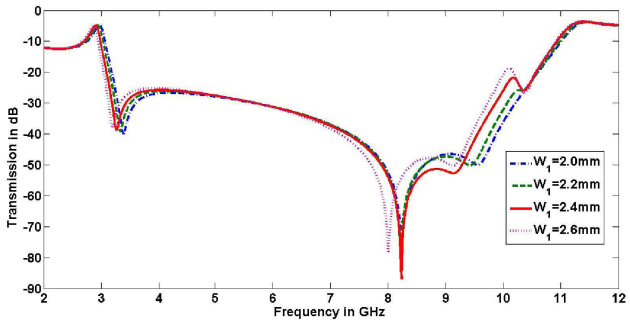

Figure 11. Effect of slot width W_1 on the transmission response of FSS ($W = 4.2$ mm, $L_1 = 3$ mm, $L_2 = 3$ mm, $W_2 = 1$ mm).

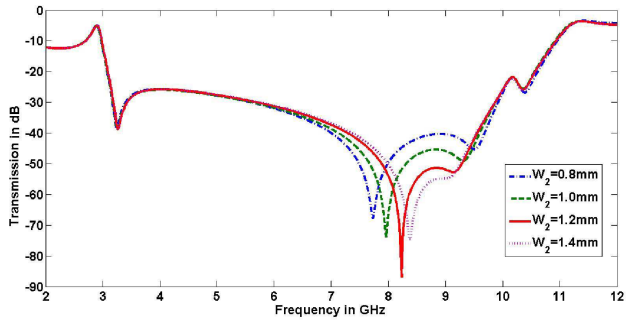

Figure 12. Effect of patch width W_2 on the transmission response of FSS ($W = 4.2\,\text{mm}$, $W_1 = 2.4\,\text{mm}$, $L_1 = 3\,\text{mm}$, $L_2 = 3\,\text{mm}$).

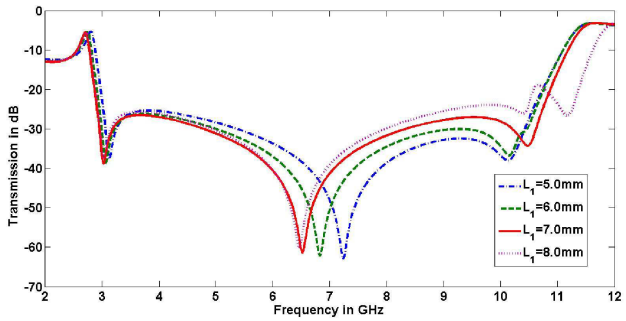

Figure 13. Effect of slot length L_1 on the transmission response of FSS ($W = 4.2\,\text{mm}$, $W_1 = 2.4\,\text{mm}$, $W_2 = 1.2\,\text{mm}$, $L_2 = 3\,\text{mm}$).

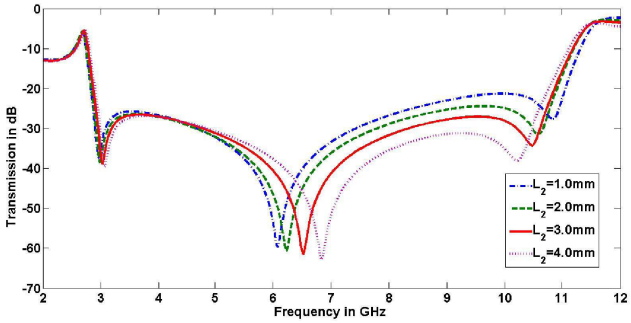

Figure 14. Effect of patch length L_2 on the transmission response of FSS ($W = 4.2\,\text{mm}$, $W_1 = 2.4\,\text{mm}$, $W_2 = 1.2\,\text{mm}$, $L_1 = 7\,\text{mm}$).

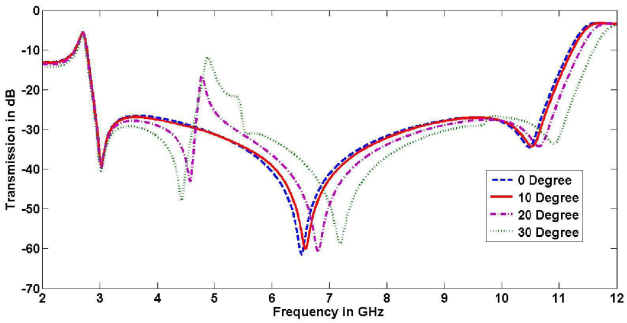

Figure 15. Effect of incident angle variation on transmission response of the proposed EBG.

FSS. The proposed FSS shows a good performance up to incident angle of 30°. It can be seen from the figure that for all the incident angles, the first resonance frequency almost remains constant. The overall bandwidth varies with a change in the incident angle. This is due to the fact that the FSS lacks rotational symmetry.

5. CONCLUSIONS

A UWB frequency selective surface is designed, investigated and experimentally validated. The proposed FSS is a two layer metallic structure. The overall thickness of the FSS is 1.8 mm which is less as compared to conventional multilayer FSS. The dimension of the unit cell is small and almost equal to the periodicity. The proposed FSS has a bandwidth of 8 GHz for incident TE waves which covers the ultra wideband region. An equivalent circuit is presented, and the resonance frequencies are also calculated. The calculated resonance frequencies are in good agreement with the simulated ones. This type of FSS structures can be used as high reflection layers for improving the gain of an antenna, in ground penetrating radar and for ultra-wideband shielding.

ACKNOWLEDGMENT

The authors would like to acknowledge Vice Chancellor, DIAT (DU), for financial support. The authors would also like to acknowledge Rajas Khokle for his help and suggestions.

REFERENCES

1. Sievenpiper, D., "High-impedance electromagnetic surfaces," Ph.D. Dissertation, Department of Electrical Engineering, University of California at Los Angeles, Los Angeles, CA, 1999.
2. Munk, B. A., *Frequency Selective Surfaces: Theory and Design,* Wiley, New York, 2000.
3. Yang, F. and Y. Rahmat Samii, *Electromagnetic Band Gap Structures in Antenna Engineering,* Cambridge University Press, 2009.
4. Chen, H.-Y. and Y. Tao, "Bandwidth enhancement of a U-slot patch antenna using dual band frequency-selective surface with double rectangular ring elements," *Microwave Opt. Technol. Lett.*, Vol. 53, No. 7, 1547–1553, Jul. 2011.
5. Monavar, F. M. and N. Komjani, "Bandwidth enhancement of microstrip patch antenna using Jerusalem cross-shaped frequency selective surfaces by invasive weed optimization approach," *Progress In Electromagnetics Research*, Vol. 121, 103–120, 2011.
6. Pirhadi, A., H. Bahrami, and J. Nasri, "Wideband high directive aperture coupled microstrip antenna design by using a FSS superstrate layer," *IEEE Transactions on Antennas and Propagation*, Vol. 60, No. 4, 2101–2106, Apr. 2012.
7. Kushwaha, N. and R. Kumar, "Design of slotted ground hexagonal microstrip patch antenna and gain improvement with FSS screen," *Progress In Electromagnetics Research B*, Vol. 51, 177–199, 2013.
8. Arnaud, E., R. Chantalat, M. Koubeissi, T. Monediere, E. Rodes, and M. Thevenot, "Global design of an EBG antenna and meander-line polarizer for circular polarization," *IEEE Antennas and Wireless Propagation Letters*, Vol. 9, 215–218, 2010.
9. Arnaud, E., R. Chantalat, T. Monediere, E. Rodes, and M. Thevenot, "Performance enhancement of self-polarizing metallic EBG antennas," *IEEE Antennas and Wireless Propagation Letters*, Vol. 9, 538–541, 2010.
10. Chiu, S.-C. and S.-Y. Chen, "High-gain circularly polarized resonant cavity antenna using FSS superstrate," *2011 IEEE International Symposium on Antennas and Propagation (APSURSI)*, 2242–2245, Jul. 3–8, 2011.
11. Winkler, S. A., W. Hong, M. Bozzi, and K. Wu, "Polarization rotating frequency selective surface based on substrate integrated waveguide technology," *IEEE Transactions on Antennas and Propagation*, Vol. 58, No. 4, 1202–1213, Apr. 2010.
12. Ranga, Y., L. Matekovits, K. P. Esselle, and A. R. Weily, "Design and analysis of frequency-selective surfaces for ultra wideband applications," *EUROCON — 2011 IEEE International Conference on Computer as a Tool (EUROCON)*, 1–4, Apr. 27–29, 2011.
13. Langley, R. J. and E. A. Parker, "Double square frequency selective surfaces and their equivalent circuit," *Electron. Lett.*, Vol. 19, No. 17, 675–677, 1983.
14. Foroozesh, A. and L. Shafai, "Investigation into the application of artificial magnetic conductors to bandwidth broadening, gain enhancement and beam shaping of low profile and conventional monopole antennas," *IEEE Transactions on Antennas and Propagation*, Vol. 59, No. 1, 4–20, Jan. 2011.
15. Jha, K. R., G. Singh, and R. Jyoti, "A simple synthesis technique of single-square-loop frequency selective surface," *Progress In Electromagnetics Research B*, Vol. 45, 165–185, 2012.
16. Sarabandi, K. and N. Behdad, "A frequency selective surface with miniaturized elements," *IEEE Transactions on Antennas and Propagation*, Vol. 55, No. 5, 1239–1245, May 2007.
17. Al-Joumayly, M. and N. Behdad, "A new technique for design of low-profile, second-order, bandpass frequency selective surfaces," *IEEE Transactions on Antennas and Propagation*, Vol. 57, No. 2, 452–459, Feb. 2009.
18. Langley, R. J. and E. A. Parker, "Equivalent-circuit model for arrays of square loops," *Electron. Lett.*, Vol. 18, No. 7, 294–296, 1982.